



## Synthesis, characterization and potential application of organobentonite in removing 2,4-DCP from industrial wastewater

Yan Zhou<sup>a</sup>, Xiao-Yin Jin<sup>a</sup>, Hongfu Lin<sup>b</sup>, Zu-Liang Chen<sup>a,\*</sup>

<sup>a</sup> School of Chemistry and Material Sciences, Fujian Normal University, Fuzhou 350007, Fujian Province, China

<sup>b</sup> Zhejiang Fenghong Clay Chemicals Co. Ltd, Anji 313300, Zhejiang Province, China

### ARTICLE INFO

#### Article history:

Received 7 July 2010

Received in revised form 22 October 2010

Accepted 22 October 2010

#### Keywords:

Adsorption

Characterization

Organobentonite

2,4-DCP

Wastewater

### ABSTRACT

Three bentonite modified with organic surfactants were used to remove 2,4-dichlorophenol (2,4-DCP) from aqueous solution. Of the three bentonites studied, DK3, modified with octadecyl dimethyl benzyl ammonium chloride (ODBAC), was found to be most effective and the conditions affecting batch adsorption of 2,4-DCP were evaluated. The adsorption data fit the Langmuir isotherm model well predicting a high adsorption capacity of 281.8 mg/g at 30 °C. A pseudo-second-order model was used to calculate the corresponding rate constant of 10.35 mg/g min<sup>-1</sup> at 30 °C. Thermodynamic parameters demonstrated that the overall adsorption process was exothermic and spontaneous. Furthermore, DK3 was characterized by scanning electronic microscopy (SEM), specific surface area (SSA), X-ray powder diffraction (XRD) and Fourier transform infrared (FTIR) spectrometer, which provided evidence of morphological properties and the adsorption of 2,4-DCP onto DK3. Finally, DK3 was used to remove >92% of 2,4-DCP from industrial wastewater having an initial concentration of 10.0 mg/L.

© 2010 Elsevier B.V. All rights reserved.

### 1. Introduction

Phenols are family of chemical pollutants that are of environmental concern because of their known toxicity and tendency to accumulate in the natural environment [1–3]. Phenolic residues have been detected worldwide in soil, water and air samples, in food products and in human and animal tissues. In recent years, several physico-chemical treatments have been proposed to remove phenol efficiently, such as adsorption, solvent extraction, wet oxidation and heterogeneous photocatalysis [1–3]. Adsorption technology is currently being used extensively to remove phenols from aqueous solutions [2,3]. For example, activated carbon is the most widely used adsorbent for the removal of a variety of organics from waters, but there are several disadvantages associated with this process that have resulted in high regeneration costs. Hence, finding alternative adsorbents that provide a cheap and effective chemical regeneration are required [4].

Natural bentonite minerals are often used as adsorbents because they are extremely cheap, being 20 times cheaper than activated carbon [3], are abundant, have high adsorption properties and have potential for ion-exchange. In recent years, interest in utilizing bentonite has increased due to its ability to simultaneously adsorb both inorganic and organic molecules. However, the adsorption capacity for apolar non-ionic organic compounds is generally

poor due to bentonite's low hydrophilicity [5]. For this reason, many studies have concentrated on the adsorptive removal of phenol and its derivatives from water using organobentonites [1–3]. Organobentonites are produced by the exchange of organic cations (typically having a quaternary ammonium and aliphatic structure) for inorganic ions (e.g., H<sup>+</sup>, Na<sup>+</sup>, Ca<sup>2+</sup>) on the surface layers of bentonites [6].

These ion exchange reactions can significantly alter the surface properties of the modified bentonite; so that the produced organic bentonites become organophilic due to the organic functional groups of the quaternary ammonium cations which are not strongly hydrated by water [1–3]. Several organobentonites have been suggested for wastewater treatment [1–3]. One organoclay was synthesized by intercalating bentonite with cetyl trimethyl ammonium bromide (CTAB) and adsorption experiments with phenol, 4-p-chlorophenol, or 2,4-DCP, together with phosphate, demonstrated that the modified clay could simultaneously remove both organics and phosphate from water mainly due to a partition and ligand exchange mechanism. Both phenol [7] and soluble organic matter [8] were removed by bentonite modified with benzyl trimethyl ammonium bromide (BTMA). Adsorption of phenol, p-chlorophenol and 2,4-DCP with hexadecyl trimethyl ammonium bromide (HDTMAB) modified bentonite [9] was also reported. Recently, adsorption of phenol and m-chlorophenol to bentonite modified with a series of cationic surfactants has shown that BTEAB-bentonite performed best, with a removal efficiency >80% for phenol and chlorophenol [10]. These results indicate that compared to natural bentonite and

\* Corresponding author. Tel.: +86 591 83465689; fax: +86 591 83465689.  
E-mail address: [zlichen@fjnu.edu.cn](mailto:zlichen@fjnu.edu.cn) (Z.-L. Chen).

**Table 1**  
Surface areas and XRD  $d(001)$  of Na-Mt and organobentonites.

Sample	XRD $d(001)$	Surface area ( $\text{m}^2/\text{g}$ )	Pore volume ( $\text{cm}^3/\text{g}$ )	Average pore diameter (nm)
Na-Mt	1.258 nm	13.70	$6.95 \times 10^{-3}$	2.03
DK1	2.314 nm	3.79	$1.74 \times 10^{-3}$	1.84
DK3	3.114 nm	6.11	$2.84 \times 10^{-3}$	1.86
DK5	1.343 nm	23.01	$1.11 \times 10^{-2}$	1.92

other clays, organobentonites are powerful adsorbents of non-ionic organics.

From recent studies of surfactant modified bentonites, it is known that the adsorption efficiency strongly depends on the type of surfactant modifying the bentonite. Therefore, the aim of this study was to prepare organobentonites using three different surfactants and to evaluate the remove efficacy of 2,4-DCP via batch adsorption studies. The corresponding kinetics, equilibrium and thermodynamic parameters were also examined. In addition, SEM, XRD and FTIR were used to characterize the organobentonite before and after adsorption. Finally, the organobentonites were used to remove 2,4-DCP from waste water to demonstrate its potential application.

## 2. Materials and methods

### 2.1. Synthesis of organically modified bentonites

The montmorillonite used in this study was Na-montmorillonite (Fenghong Co. Ltd., Jian, Zhejiang, China) having a cation exchange capacity (CEC) of 75.40 mequiv/100 g. The chemical composition of the montmorillonite was 62.50%  $\text{SiO}_2$ , 18.50%  $\text{Al}_2\text{O}_3$ , 1.75%  $\text{Fe}_2\text{O}_3$ , 4.25%  $\text{MgO}$ , 0.95%  $\text{CaO}$ , and 2.75%  $\text{Na}_2\text{O}$ . The three surfactants, octadecyl dimethyl benzyl ammonium chloride, hexadecyltrimethylammonium and aminocaproic acid, as well as 2,4-DCP, were all analytical grade reagents and used without further purification. A solution containing 2,4-DCP was prepared by dissolving 2,4-DCP with deionized water to the desired concentration. It was then stored in the refrigerator for one month prior to use. The final pH of the solution was adjusted using 0.10 mol/L, NaOH and HCl. The organobentonites modified with hexadecyltrimethylammonium, octadecyl dimethyl benzyl ammonium chloride and aminocaproic acid will hereafter be referred to as DK1, DK3 and DK5, respectively.

The Na-montmorillonite (Na-Mt) was initially dispersed in deionized water with magnetic stirring at 600 rpm for 3 h. Subsequent Na-Mt suspension (50 g) was added into a cationic surfactant solution and the mixture was stirred on a water bath at 80 °C for 150 min in order to avoid frothing. The ratio of cationic surfactant solution to the bentonite was 20% (w/w). The suspension was subsequently washed with distilled water 4 times. The moist solid material was dried in an oven at 60 °C and ground with a mortar. The montmorillonite content in the organic bentonite ranged from 96% to 98% with a measured diameter <75  $\mu\text{m}$ . The lamellar distance was less than 2.50 nm, and the apparent density was 0.30 g/cm<sup>3</sup>.

### 2.2. Characterization

Solid morphology of the original clay (Na-Mt) and the modified clay (DK3) was determined using a scanning electron microscope (SEM) (JSM 7500F, Japan). The specific surface areas (SSA) of Na-Mt and organobentonites (Table 1) were measured using the BET-N<sub>2</sub> adsorption method (the Brunauer–Emmett–Teller isotherm) on a Micromeritics' ASAP 2020 Accelerated Surface Area and Porosimetry Analyzer (Micromeritics Instrument Corp., GA) using the gas sorption technique. The crystal characteristics of the Na-Mt and organobentonites were investigated using an X-ray diffraction

(XRD) instrument (X' Pert Pro MPD, Netherlands) with filtered Cu K $\alpha$  radiation operated at 40 kV and 40 mA. The XRD pattern was recorded from 1.50° to 30° of  $2\theta$  with a scanning speed of 0.02° of  $2\theta$  per second. The infrared spectra of both the Na-Mt and modified clay minerals were obtained by Fourier transform infrared spectroscopy (FTIR Nicolet 5700, Thermo Corp., U.S.A). Samples for FTIR measurement were prepared by mixing 1% (w/w) specimen with 100 mg of KBr powder and pressed into a sheer slice. An average of 9 scans was collected for each measurement with a resolution of 2  $\text{cm}^{-1}$ .

### 2.3. Adsorption experiments and removal of 2,4-DCP from wastewater

To compare the adsorption capacity of the synthesized organobentonites, organo bentonite (0.25 g) was placed in a 50 mL plastic tube containing an aqueous solution of 500 mg/L 2,4-DCP (25 mL) and the solutions shaken at 250 rpm at 30 °C. Organically modified clay DK3 (0.3 g) was combined with 2,4-DCP solutions of different concentration (25 mL) in 50 mL Erlenmeyer flasks with plastic caps. Various experimental conditions, including contact time, pH, adsorbent dosage, initial concentration and temperature, were tested for their effect on 2,4-DCP adsorption from solution. After equilibration all adsorption solutions were centrifuged at 3500 rpm for 10 min and the 2,4-DCP concentration in the aqueous phase determined using a UV-260 spectrophotometer at 286 nm.

Real wastewater was collected from a ceramics factory in Min Qing in Fujian, China where the concentrations of 2,4-DCP were 102 and 5.5 mg/L. For wastewater samples, DK3 (0.25 g) was mixed with wastewater (25 mL) containing different concentration of 2,4-DCP.

The 2,4-DCP removal rate onto the organoclays was calculated using the equation  $R = (C_0 - C_e)/C_0 \times 100\%$ , where:  $R$  is the phenol removal rate;  $C_0$  is the initial concentration; and  $C_e$  is the equilibrium concentration of the 2,4-DCP [11]. Blank experiments (without adsorbent) were carried out in parallel. All experiments were carried out in duplicate.

### 2.4. The determination of $\text{pH}_{\text{pzc}}$

Batch equilibrium experiments were used to estimate zero point charge ( $\text{pH}_{\text{pzc}}$ ). DK3 (0.2 g) was added into a background electrolyte of 0.01 M NaCl (100 mL). The initial pH ( $\text{pH}_{\text{initial}}$ ) was then adjusted from 2 to 12 by adding minute amounts of either 0.01 M NaOH or 0.01 M HCl. The suspensions were equilibrated at room temperature for 24 h in a rotary shaker at 200 rpm and thereafter filtered and the final pH ( $\text{pH}_{\text{final}}$ ) of the filtrate determined. A plot of final pH as a function of the initial pH allowed  $\text{pH}_{\text{pzc}}$  of the adsorbent to be determined from the plateau of constant pH on the ordinate axis.

## 3. Results and discussion

### 3.1. The removal of 2,4-DCP using various organobentonites

The removal percentages of 2,4-DCP were 99.3, 92.8, 60.6 and 14.0% for DK3, DK1, DK5 and Na-Mt, respectively (Fig. 1). The results showed that the best adsorption capacity for 2,4-DCP from aqueous solution occurred when using DK3, while poorest removal

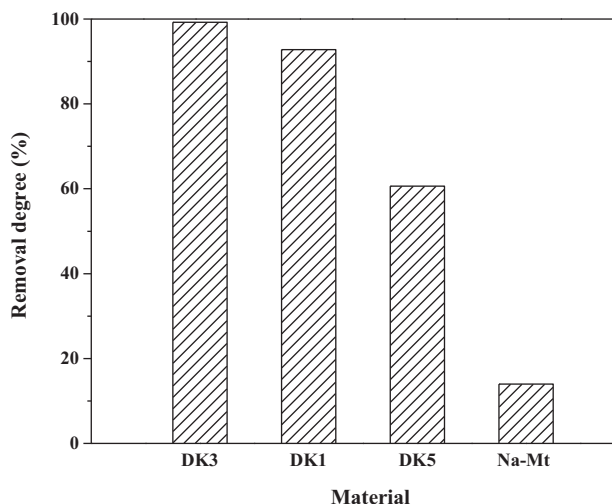


**Fig. 1.** Percentage of 2,4-DCP removal by different sorbents. Dosage: 10 g/L; pH: initial pH; equilibration time: 60 min; rotary speed: 250 rpm and temperature: 30 °C. Initial concentration: 500 mg/L.

efficiency was observed using Na-Mt indicating that removal of 2,4-DCP. Using a modified organobentonite was more effective than unmodified montmorillonite. This was due to the expansion of the montmorillonite interlayers after surfactant modification [6,12], as observed in the X-ray diffraction patterns (Table 1), where the values of  $d(001)$  basal spacing increased in the order: 1.258 nm (Na-Mt)  $\rightarrow$  1.343 nm (DK5)  $\rightarrow$  2.314 nm (DK1)  $\rightarrow$  3.114 nm (DK3). With the exception of DK5, the specific surface area before modification was higher than modified bentonites (Table 1). The removal percentages of 2,4-DCP increased with increasing  $d(001)$  spacing. Increased organophilicity is the main reason for the observed increases in 2,4-DCP removal efficiency [5]. Since the determined basal spacings of all tested samples exceeded the molecular diameter of 2,4-DCP, indicating that 2,4-DCP replaced some of the surfactant cations within the clay interlayer and were easily absorbed onto the surface of DK3 due to DK3's high interlayer space and high organophilic character. Therefore, the adsorption of 2,4-DCP onto organobentonite was in the order of effectiveness of: DK3 > DK1 > DK5 > Na-Mt.

### 3.2. Characterization

#### 3.2.1. SEM

The SEM micrographs of both Na-Mt (a) and DK3 (b) are shown in Fig. 2. The SEM micrographs of Na-Mt highlight the shape of

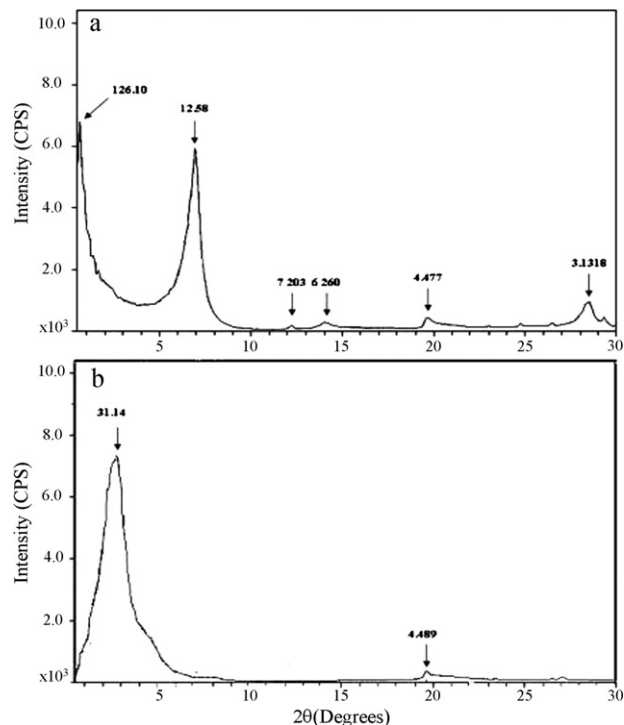


**Fig. 3.** XRD patterns of Na-Mt (a) and DK3 (b).

organobentonite (OB) as an irregular phenomenon, where the surface was unsmooth due to granule impurities. The surface morphology of DK3 was smoother than that of Na-Mt after modification with smaller fragments and a clearer sheet structure.

#### 3.2.2. XRD

Expansion of the montmorillonites can be observed using X-ray powder diffraction. Fig. 3 shows the XRD patterns of Na-Mt and DK3. The basal spacing for Na-Mt was 1.258 nm, representing the typical XRD pattern of pristine Na-Mt with the  $d(001)$  plane reflection peak at about 6° (two theta). This corresponds to the basal spacing with coordinating Na<sup>+</sup> and Ca<sup>2+</sup> ions in the interlayer space with one molecular water layer (3.114 nm). However, for DK3, the  $d(001)$  spacing increased to 3.114 nm with modification by surfactant, indicating that ODBAC<sup>+</sup> cations had been intercalated into the montmorillonite interlayer space. This was attributed to the surfactant molecular arrangement laying flat in the interlayer space, leading to expansion of the interlayer space

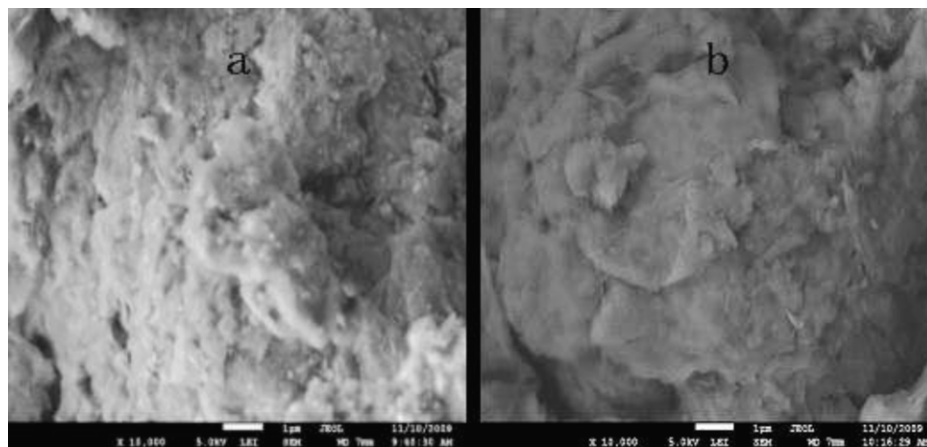


**Fig. 2.** SEM scanning images of Na-Mt (a) and DK3 (b).

**Table 2**

Isotherm parameters at various temperatures for different isotherm models of adsorption 2,4-DCP by DK3.

Temperature (K)	Freundlich isotherm			Langmuir isotherm		
	$K_F$	$1/n$	$R^2$	$q_m$ (mg/g)	$K_L$ (L/mg)	$R^2$
303	19.27	0.605	0.989	281.80	0.1335	0.9971
308	19.26	0.605	0.987	180.70	0.1332	0.9972
313	19.24	0.607	0.984	150.50	0.1331	0.9965

$R^2$  = correlation coefficient.

[13,14]. As shown in Table 2, after modification the basal spacing of both DK1 and DK5 increased to 2.314 and 1.343 nm, respectively. The difference was due to the size of the surfactant molecules. The observation suggests that surfactant molecules intercalate into the montmorillonite interlayer [13,14].

### 3.2.3. FTIR

The FTIR spectra of the Na-Mt and DK3 (without and with adsorption of the 2,4-DCP) were recorded in wave numbers ranging from 400 to 4000  $\text{cm}^{-1}$  (Fig. 4). The bands of Na-Mt at 1041 and 919  $\text{cm}^{-1}$  are attributed to Si-O and Al-O bending vibrations, respectively [15]. The bands at 464, 519 and 3628  $\text{cm}^{-1}$  are attributed to Al-O-Si stretching vibration and stretching vibration of structural OH groups in bentonite. The bands at 1467 and 1487  $\text{cm}^{-1}$  correspond to ammonium ions, and the bands at 2923 and 2852  $\text{cm}^{-1}$  are due to the symmetric and antisymmetric  $\text{CH}_2$  stretching vibration [16]. In the 2,4-DCP spectrum it was possible to observe a strong O-H band centered at 3445  $\text{cm}^{-1}$  (typical of phenylic acid), a C=C band centered at 1500 and 1580  $\text{cm}^{-1}$  (due to C=C aromatic ring stretching), a C-Cl band centered at 725  $\text{cm}^{-1}$  in the fingerprint region. These characteristic peaks can be found in DK3 after binding with 2,4-DCP. This may have been caused by the reaction between the surfactant of DK3 with 2,4-DCP and provides evidence of 2,4-DCP linkage with the DK3. These results therefore suggest that ODBAC<sup>+</sup> cations had been intercalated into the montmorillonite interlayer space and 2,4-DCP molecules were subsequently adsorbed on DK3 via interaction with the surfactant.

### 3.3. Equilibrium studies

#### 3.3.1. Effect of contact time

The effect of contact time on the adsorption capacity of DK3 was investigated for contact times between 5 and 50 min at pH of

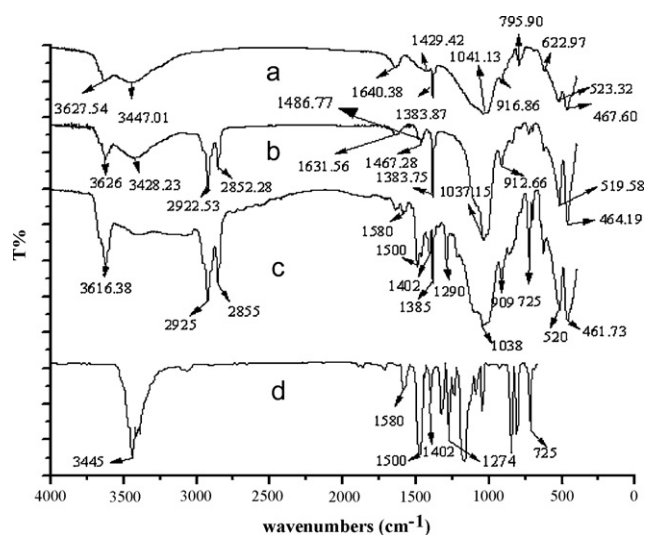


**Fig. 4.** FTIR spectral of Na-Mt (a), DK3 (b), DK3 with 2,4-DCP adsorbed (c) and 2,4-DCP (d).

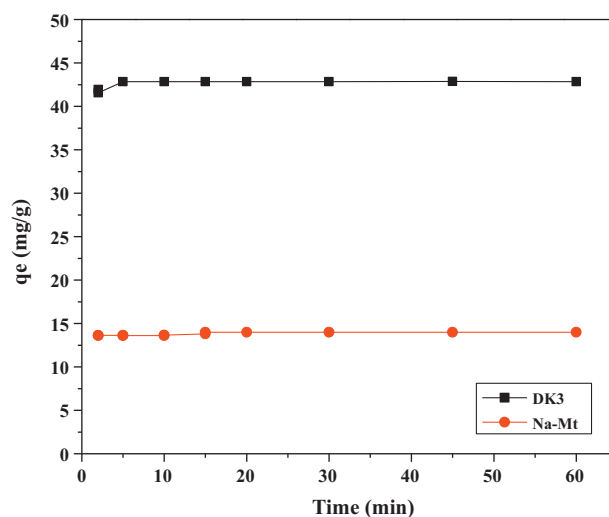


**Fig. 5.** Effect of time. Dosage: 10 g/L; pH: initial pH; rotary speed: 250 rpm and temperature: 30 °C. Initial concentration: 500 mg/L.

6.0 at 30 °C. Initial adsorption of 2,4-DCP was rapid for both DK3 and Na-Mt, and 2,4-DCP-DK3 interactions reached equilibrium in less than 5 min (Fig. 5). Thus, the contact time of 60 min was used in the following sections. The adsorption sites on the clay minerals were quickly covered by the 2,4-DCP and the adsorption rate depended on the rate at which the 2,4-DCP was transported from the bulk liquid phase to the actual adsorption sites [13]. However, unlike the unmodified Na-Mt, there was a significant increase in the adsorption of 2,4-DCP on DK3 due to its larger interlayer space and higher organophilic character [14,17]. Clearly, DK3 significantly enhanced adsorption of 2,4-DCP. For example, the amount of 2,4-DCP adsorbed by natural Na-Mt was less than 14 mg/g, while the amount adsorbed by DK3 was nearly 42.8 mg/g. This indicates that the adsorption of 2,4-DCP on DK3 depended not only on the partition mechanism but was also significantly influenced by the hydrocarbon chain length, degree of exchangeable cation replacement by surfactant molecules and the number of hydrocarbon chains within the surfactant molecule [18].

#### 3.3.2. Effect of absorbent dosage

The adsorption percentage and adsorption capacity ( $q_e$ ) for 2,4-DCP was a function of DK3 dosage at the given conditions (Fig. 6). The phenol adsorption percentage increased from 70.6 to 99.8%

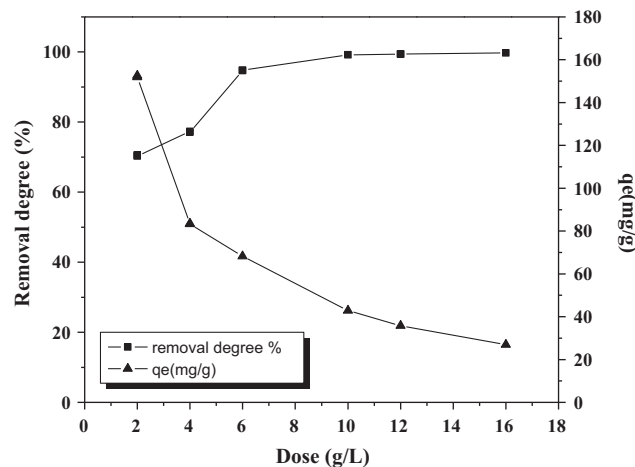


**Fig. 6.** Effect of absorbent dosage. Equilibration time: 60 min; pH: initial pH; rotary speed: 250 rpm and temperature: 30 °C. Initial concentration: 500 mg/L.

and the adsorption capacity decreased from 151.85 to 26.93 mg/g as adsorbent dosage increased from 1 to 16 g/L. This was due to the number of available adsorption sites increasing with adsorbent dosage, resulting in a higher adsorption capacity [19]. This is mainly attributed to the effect of the interactions between the particles [19], such as aggregation leading to an increase in diffusion path length and a decrease in total surface area of the adsorbent. With increasing DK3 dosage from 10 to 16 g/L, the phenol adsorption percentage only increased slightly. Therefore, 10 g/L adsorbent dosage was sufficient for all subsequent experiments as little increase would have been gained using larger amounts of adsorbent.

### 3.3.3. Effect of pH

The effect of pH on 2,4-DCP removal was investigated in the pH range 2–6 at 30 °C when equilibrated for 1 h. The highest adsorption of 2,4-DCP on DK3 was obtained at pH 6. When pH increased from 2.0 to 6.5, the amount of 2,4-DCP adsorbed increased from 42.4 to 44.8 mg/g, and then decreased with further increases in the pH from 6.5 to 12.0 (to 42.5 mg/g). The adsorption of 2,4-DCP on DK3 may be explained by three main mechanisms. At  $\text{pH} > \text{pKa}$  (7.85) electrostatic attraction between DK3 occurs when 2,4-DCP is in the anionic form. As ionization of 2,4-DCP increases with increases in solution pH, this leads to a decrease in the adsorption of 2,4-DCP on DK3 [20]. When the pH values are  $> \text{pH}_{\text{pzc}}$  6.5, the surface of DK3 is negatively charged, leading to a decrease in adsorption efficiency because of repulsion between 2,4-DCP and DK3. Secondly, some 2,4-DCP would be ionized by hydrolysis when the pH was 6.5. The maximum adsorption efficiency is the result of the partition process and ion exchange. When the solution pH is  $< \text{pKa}$  [21] 2,4-DCP exists in molecular form and is adsorbed on DK3 by Van der Waals attractions to alkyl chains [6,18]. However, the results showed that in this study the solution pH did not significantly affect the adsorption of 2,4-DCP onto DK3 and therefore a solution pH of 6.5 was used in the following sections.

### 3.3.4. Effect of the initial concentration and temperature

The initial 2,4-DCP concentration in the range 100–5000 mg/L influenced the adsorption of 2,4-DCP on the DK3 when the pH was 6.5 and temperature was either 30, 35 or 40 °C when equilibrated for 1 h (Fig. 7). Initial increases in 2,4-DCP concentration resulted in an increase in 2,4-DCP adsorption by DK3. The removal percentage of 2,4-DCP increased rapidly with an increase in 2,4-DCP concentration from 100 to 1500 mg/L, but increased more

slowly and approached a plateau when the 2,4-DCP concentration reached 3000 mg/L. With increases in 2,4-DCP concentration above 3000 mg/L there was an increase in the amount of 2,4-DCP adsorbed by DK3. This was due to the initial phenol concentration providing an important driving force to overcome all mass transfer limitations of phenol between the aqueous and solid phases. In addition, the other main consequence of reaching partition equilibrium was the portion of adsorbed molecules depended on the given conditions and on the initial adsorbate concentration and the partition coefficient, with the number of available adsorption sites being a limiting factor.

Therefore, a higher initial phenol concentration will enhance the adsorption process [22]. When the 2,4-DCP concentration was 3000 mg/L, the amount of 2,4-DCP adsorbed by DK3 was 202 mg/g at 35 °C. However, there was no distinct difference in  $q_e$  values when the initial phenol concentrations were higher than 3000 mg/L which indicated that the adsorption reached saturation at a high phenol concentration due to a limited number of surface binding sites.

Fig. 7 also shows the effect of the initial 2,4-DCP concentration on the equilibrium adsorption capacity ( $q_e$ ) and adsorption percentage of 2,4-DCP on the DK3 at different temperatures. While  $q_e$  was not significantly affected by the temperature when initial 2,4-DCP concentration varied from 100 to 1500 mg/L, when the 2,4-DCP concentration increased from 1500 to 3000 mg/L, the adsorption of 2,4-DCP on the DK3 depended primarily on temperature. For example, the  $q_e$  for 2,4-DCP decreased from 175 to 235 mg/g at an initial concentration of 3000 mg/L when the temperature increased from 30 °C to 40 °C. The maximum equilibrium  $q_e$  values were determined as 231, 202 and 186 mg/g at an initial phenol concentration of 3000 mg/L at 30, 35 and 40 °C, respectively. The decrease in adsorption capacity and adsorption percentage when temperatures rose was due to increasing adsorption of the 2,4-DCP onto the DK3. This also indicated that the adsorption of 2,4-DCP on the DK3 was endothermic and involved both physical and chemical sorption [3,23].

### 3.3.5. Desorption of the 2,4-DCP

The successful use of an adsorbent for wastewater treatment depends not only on the adsorptive capacity, but also on how well the adsorbent can be regenerated and subsequently re-used [3]. In this study, desorption of 2,4-DCP from DK3 was carried out in batch experiments. Deionized water (30 mL) was added to DK3 (0.2 g) saturated with 2,4-DCP. The suspension was then shaken for 10 min, filtered and the filtrate analysed for 2,4-DCP content. As shown in Fig. 8, less than 1% of 2,4-DCP was desorbed from DK3, within 60 min and remained constant thereafter. The lack of significant desorption indicated that there were strong bonds between 2,4-DCP, and the binding sites of DK3 and that 2,4-DCP was likely adsorbed and penetrated into the interlayer space of DK3 [12].

## 3.4. Adsorption studies

### 3.4.1. Adsorption isotherms

Most adsorption data can be adequately expressed by either the Langmuir or Freundlich models. The Langmuir isotherm is expressed as follows [1–3]:

$$\frac{C_e}{q_e} = \frac{C_e}{q_0} + \frac{1}{q_0 K} \quad (1)$$

where  $q_e$  (mg/g) is the adsorption capacity at equilibrium;  $q_0$  (mg/g) is the maximum adsorption capacity;  $C_e$  (mg/L) is the equilibrium concentration of 2,4-DCP; and  $K$  (L/mg) is a constant related to the adsorption energy.

Based on further analysis of the Langmuir equation, the dimension parameter of the equilibrium or adsorption intensity ( $R_L$ ) can

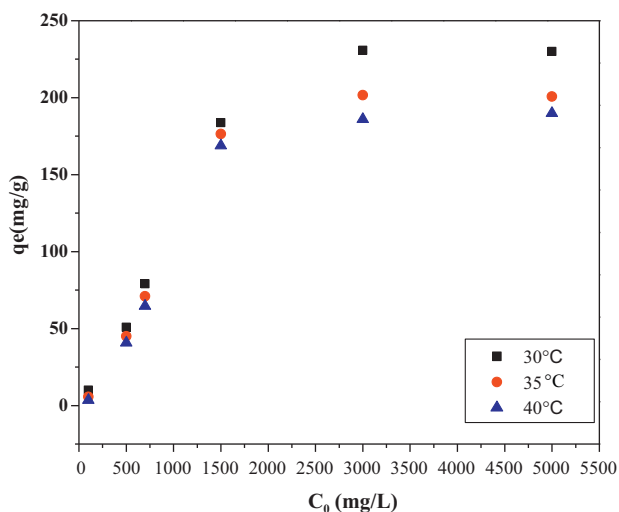


Fig. 7. Effect of the initial concentration and temperature. pH: initial pH; dosage: 10 g/L; contacting time: 60 min.

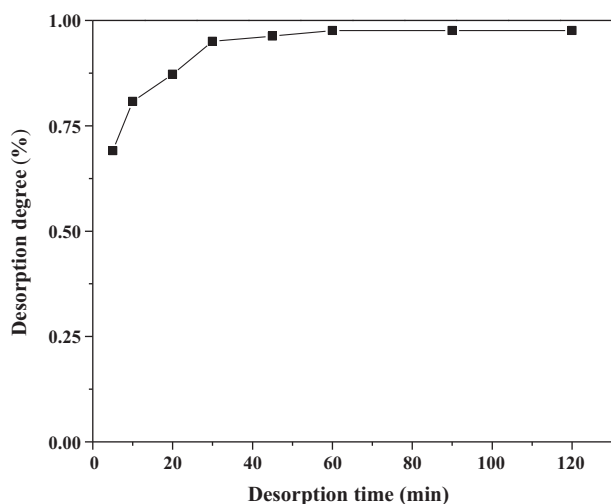


Fig. 8. Relationship between desorption time and desorption rate.

be expressed as [1]:

$$R_L = \frac{1}{1 + KC_0} \quad (2)$$

where  $C_0$  (mg/L) is the initial concentration of 2,4-DCP and  $R_L$  is considered to be the indicator of adsorption. The value of  $R_L$  indicates the type of isotherms: for unfavourable adsorption,  $R_L > 1$ ; for linear adsorption,  $R_L = 1$ ; for favourable adsorption,  $0 < R_L < 1$ ; and for irreversible adsorption,  $R_L = 0$ .

The Freundlich isotherm model is an empirical equation valid for adsorption on the assumption that process occurs on heterogeneous surfaces [2,3]. The Freundlich isotherm equation is expressed as:

$$\ln q_e = \ln K_F + \frac{1}{n} \ln C_e \quad (3)$$

where  $K_F$  is the Freundlich constant associated with the relative capacity and  $n$  relates to the adsorption intensity.

The constants of the Freundlich and Langmuir isotherms were obtained from the slope and intercept of the plots for each isotherm at different temperatures (Table 2). The  $R^2$  values all exceeded 0.98 for both the Freundlich and Langmuir models suggesting that both models closely fit the experimental data. With respect to the coefficients of the Langmuir model, the values of  $K_L$  were 0.1335, 0.1332 and 0.1331 L/mg at 30, 35 and 40 °C, respectively.  $K_L$  increased as temperatures fell, indicating that the affinity of binding sites for 2,4-DCP decreased at higher temperature, and the values of  $R_L$  ranged between 0 and 1, also suggesting that the adsorption of 2,4-DCP by DK3 was favourable [2]. In addition,  $R_L$  decreased from 0.07 to 0.0015 as the  $C_0$  increased from 100 to 5000 mg/L (Fig. 9). The magnitude of variation in  $R_L$  ( $0 < R_L < 1$ ) indicated that the adsorption of 2,4-DCP by DK3 was favourable and that DK3 was a suitable adsorbent for removing 2,4-DCP from aqueous solution [9].

In the Freundlich model, Freundlich constant ( $K_F$ ) and the heterogeneity factor ( $1/n$ ) calculated from the slope and the intercept of the linear plot were 19.27, 19.26, 19.24 mg/g and 0.605, 0.605, 0.607, respectively. Since the value of  $1/n$  was less than 1, this suggested that the adsorption of 2,4-DCP on the DK3 was a physical process [24]. The values  $1/n$  between 0.605 and 0.607 indicated favourable adsorption and a high affinity of DK3 for 2,4-DCP since the higher value of  $1/n$  corresponded to greater heterogeneity of the adsorbent surface [25] which resulted from 2,4-DCP interactions with surfactant cations on the clay's surface as well as within the clay interlayer space [6,18]. Therefore, both the Freundlich and Langmuir models suggest that the adsorption capacity increased as

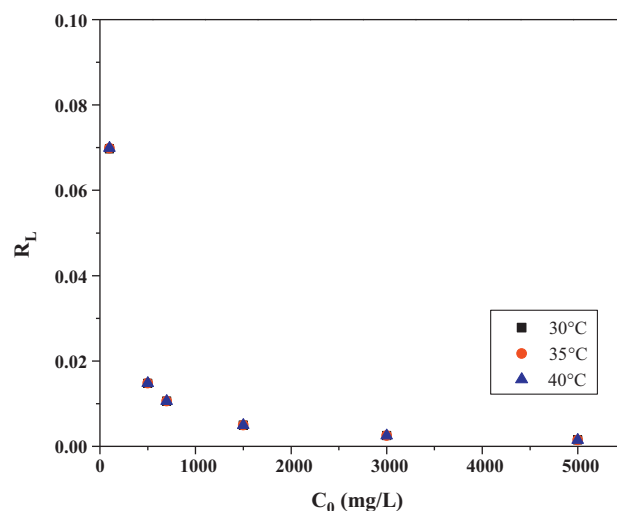


Fig. 9. Variation of separation factor ( $R_L$ ) as a function of initial 2,4-DCP concentration.

the temperature fell, demonstrating that adsorption was exothermic [26] and both models as indicated by  $R^2$  values (Table 2) fit the data well. The Langmuir and Freundlich constants both suggested that DK3 had a high capacity for absorbing 2,4-DCP from aqueous solution.

### 3.4.2. Adsorption kinetics

The pseudo-second-order kinetic model was used to describe the adsorption mechanism. It can be expressed by the following equation [2]:

$$\frac{t}{q_t} = \frac{1}{K_2 q_e^2} + \frac{t}{q_e} \quad (4)$$

where  $q_e$  is the maximum adsorption capacity (mg/g) of 2,4-DCP,  $q_t$  (mg/g) is the adsorption capacity at equilibrium time  $t$  (h), and  $k_2$  (g/(mg h)) represents the rate constant of the adsorption. Values of  $k_2$  and  $q_e$  can be calculated from the plot of  $t/q_t$  against  $t$ . The initial adsorption rate  $h$  (mg/(g h)) can be obtained according to the following equation [2,3]:

$$h = k_2 \times Q_2^2 \quad (5)$$

Table 3 shows the pseudo-second-order rate constants for the adsorption of 2,4-DCP on the DK3 at various temperatures. The linear correlation coefficient  $R^2$  derived from each temperature was more than 0.998 which clearly showed that the pseudo-second-order kinetic model described the adsorption behavior of 2,4-DCP on the DK3 well. This suggested that the adsorption mechanism may be chemical rather than physical, which was the main rate-controlling step throughout the adsorption process [27]. The amount of 2,4-DCP adsorbed at equilibrium decreased from 69.5 to 61.7 mg/g as the temperature rose. However, increases in temperatures from 30 to 40 °C resulted in only a slight increase in the rate constant,  $k$ , from 0.0022 to 0.0029 g/mg min<sup>-1</sup>. In addition, the initial adsorption rate  $h$  also increased from 10.3 to 10.9 mg/g min<sup>-1</sup> when the temperature increased from 30 to 40 °C. These results

Table 3  
Pseudo-second-order parameters obtained from the adsorption of the 2,4-DCP and DK3 under different experimental conditions.

Temperature (K)	$R^2$	$q_e$ (mg/g)	$k_2$ (g/mg min <sup>-1</sup> )	$h$ (mg/g min <sup>-1</sup> )
303	0.9989	68.49	0.0022	10.30
308	0.9989	63.29	0.0026	10.35
313	0.9982	61.73	0.0029	10.93

**Table 4**  
Thermodynamic parameters for the adsorption of 2,4-DCP by DK3.

	$\Delta H^\circ$ (kJ/mol)	$\Delta S^\circ$ (J/K mol)	$\Delta G^\circ$ (kJ/mol)			
			298 K	303 K	308 K	313 K
DK3	-65.31	-197.35	-4.58	-3.83	-2.98	-2.12

**Table 5**  
Removal of 2,4-DCP from actual wastewater.

2,4-DCP concentration	Wastewater	
Initial (mg/L)	102	5.50
Final (mg/L)	8.16	0.21
Removal rate (%)	92.0%	96.3%

indicated that adsorption of 2,4-DCP was not favourable at a high temperature. Increase in temperature causes an increase in the mobility of 2,4-DCP. However, when temperature increased further, the kinetic energies of 2,4-DCP became higher than the potential attractive forces of the active sites on the surface of the adsorbent [27], leading to a decrease in the adsorption of 2,4-DCP on the DK3.

#### 3.4.3. Thermodynamic study

Thermodynamic parameters such as standard free energy change ( $\Delta G^\circ$ ), standard enthalpy change ( $\Delta H^\circ$ ) and standard entropy change ( $\Delta S^\circ$ ) can be calculated using the following equation [3]:

$$\ln K_c = -\frac{\Delta G^\circ}{RT} = \frac{\Delta S^\circ}{R} - \frac{\Delta H^\circ}{RT} \quad (6)$$

where  $K_c$  is the equilibrium constant resulting from the ratio of the equilibrium concentrations of the phenol on an adsorbent in the solution.  $\Delta G^\circ$ ,  $\Delta H^\circ$  and  $\Delta S^\circ$  can be calculated from a plot of  $\ln K_c$  versus  $1/T$ .

Table 4 summarizes the thermodynamic parameters at various temperatures for the adsorption of 2,4-DCP onto DK3. The negative values of enthalpy  $-\Delta H^\circ$ ,  $-65.31$  kJ/mol indicated that the adsorption of 2,4-DCP using DK3 was exothermic, while the negative  $\Delta S^\circ$  values of  $-197.35$  J/(K mol) revealed decreasing randomness at the solid/solution interface during the adsorption of 2,4-DCP [28]. The obtained negative Gibbs free enthalpy ( $\Delta G^\circ$ ) values were  $-4.58$ ,  $-3.83$ ,  $-2.98$  and  $-2.12$  kJ/mol at 25, 30, 35 and 40 °C, respectively. The  $\Delta G^\circ$  values were negative at all of the tested temperatures, confirming that the adsorption of 2,4-DCP on the DK3 was spontaneous and thermodynamically favourable [18]. In addition, a more negative  $\Delta G^\circ$  implied a greater driving force of adsorption, resulting in a higher adsorption capacity. Furthermore, an increase in Gibbs energy with increasing temperature suggested that the adsorption of 2,4-DCP on the DK3 was less favourable at higher temperatures [28].

#### 3.5. Removal of 2,4-DCP from industrial wastewater

In this study, DK3 was used as an adsorbent to remove 2,4-DCP from industrial wastewater, which was collected from a ceramics industry at Min Qing in Fujian, China. The results obtained from wastewaters containing different concentrations of 2,4-DCP are summarized in Table 5. The initial concentrations of 2,4-DCP were 102 and 5.5 mg/L, respectively. However, a 0.25 g DK3 was added to 25 mL of wastewater, and then the tubs were shaken at 30 °C and 250 rpm for 1 h. As shown in Table 5, the concentrations of 2,4-DCP declined from 102 to 8.16 mg/L and 5.5 to 0.21 mg/L, where the removal percentages were 92 and 99.6%, respectively. The primary results show that DK3 has the potential to be an adsorbent that can remove 2,4-DCP from industrial wastewater.

## 4. Conclusion

The results obtained in this study show that DK3 has the potential to be a highly effective and efficient adsorbent for removing 2,4-DCP from wastewater. Both the Freundlich and Langmuir isotherm models fit the experiment data well, suggesting that the adsorption was exothermic. However, the correlation coefficient value of the linear plot for the Langmuir isotherm was better suited when the adsorption capacity reached 281.8 mg/g at 30 °C. The pseudo-second-order kinetic model best described the adsorption behavior of 2,4-DCP onto DK3, suggesting that the adsorption mechanism may be chemical rather than physical, which was the main rate-controlling step throughout the adsorption process. Results for the thermodynamic study show that the adsorption of 2,4-DCP on the DK3 was spontaneous and endothermic. Furthermore, the results obtained from both XRD and FTIR suggested that the surfactant molecules intercalated into the interlayers of montmorillonite and that ODBAC<sup>+</sup> cations had been intercalated into the montmorillonite interlayer space. Finally, the mechanism for the adsorption of 2,4-DCP on the DK3 includes the partition mechanism, the 2,4-DCP was able to replace some of the surfactant cations within the clay interlayer and be easily absorbed within the surface of the DK3.

## Acknowledgements

This research was supported by a Fujian “Minjiang Fellowship” Grant from Fujian Normal University. The authors gratefully acknowledge the significant scientific contributions made by Dr Gary Owens in revising this manuscript during the review process.

## References

- [1] G. Buscaa, S. Berardinelli, C. Resini, L. Arrighib, Technologies for the removal of phenol from fluid streams: a short review of recent developments, *J. Hazard. Mater.* 160 (2008) 265–288.
- [2] Md. Ahmaruzzaman, Adsorption of phenolic compounds on low-cost adsorbents: a review, *Adv. Colloid Interface Sci.* 143 (2008) 48–67.
- [3] S.H. Lin, R.S. Juang, Adsorption of phenol and its derivatives from water using synthetic resins and low-cost natural adsorbents: a review, *J. Environ. Manage.* 90 (2009) 1336–1349.
- [4] A. Kuleyin, Removal of phenol and 4-chlorophenol by surfactant-modified natural zeolite, *J. Hazard. Mater.* 144 (2007) 307–315.
- [5] G.J. Churchman, W.P. Gates, B.K.G. Theng, G. Yuan, Clays and clay minerals for pollution control, *Handb. Clay Sci.* 1 (2006) 625–675.
- [6] L. Zhu, R. Zhu, Simultaneous sorption of organic compounds and phosphate to inorganic–organic bentonites from water, *Sep. Purif. Technol.* 54 (2007) 71–76.
- [7] Y. Shen, Removal of phenol from water by adsorption–flocculation using organobentonite, *Water Res.* 36 (2002) 1107–1114.
- [8] Y. Shen, Removal of dissolved organic matter from water by adsorption–flocculation using organobentonite, *Environ. Technol.* 23 (2002) 553–560.
- [9] Z. Rawajfih, N. Nsour, Characteristics of phenol and chlorinated phenols sorption onto surfactant-modified bentonite, *J. Colloid Interface Sci.* 298 (2006) 39–49.
- [10] S. Lin, M. Cheng, Adsorption of phenol and m-chlorophenol on organobentonites and repeated thermal regeneration, *Waste Manage.* 22 (2002) 595–603.
- [11] Q. Fu, Y. Deng, H. Li, J. Liu, H. Hu, S. Chen, T. Sa, Equilibrium, kinetic and thermodynamic studies on the adsorption of the toxins of *Bacillus thuringiensis* subsp. *kurstaki* by clay minerals, *Appl. Surf. Sci.* 255 (2009) 4551–4557.
- [12] L. Zhu, Y. Li, J. Zhang, Sorption of organobentonites to some organic pollutants in water, *Environ. Sci. Technol.* 31 (1997) 1407–1410.
- [13] Y. Li, X. Li, Y. Li, J. Qi, J. Bian, Y. Yuan, Selective removal of 2,4-dichlorophenol from contaminated water using non-covalent imprinted microspheres, *Environ. Pollut.* 157 (2009) 1879–1885.
- [14] Y. Xi, R. Frost, H. He, Modification of the surfaces of Wyoming montmorillonite by the cationic surfactants alkyl trimethyl, dialkyl dimethyl, and trialkyl methyl ammonium bromides, *J. Colloid Interface Sci.* 305 (2007) 150–158.
- [15] R. Frost, H.P. He, W. Shen, P. Yuan, Q. Zhou, J.X. Zhu, Mechanism of p-nitrophenol adsorption from aqueous solution by HDTMA<sup>+</sup>-pillared montmorillonite-implications for water purification, *J. Hazard. Mater.* 154 (2008) 1025–1032.
- [16] M. Akcay, Characterization and adsorption properties of tetrabutylammonium montmorillonite (TBAM) clay: thermodynamic and kinetic calculations, *J. Colloid Interface Sci.* 296 (2006) 16–21.
- [17] P. Yuan, F. Annabi-Bergayab, Q. Tao, M. Fana, Z. Liud, J.X. Zhua, H.P. Hea, T. Chene, A combined study by XRPD, FTIR, TG and HRTEM on the structure of

- delaminated Fe intercalated/pillared clay, *J. Colloid Interface Sci.* 324 (2008) 142–149.
- [18] B. Witthuhn, T. Pernyeszi, P. Klauth, H. Vereecken, E. Klumpp, Sorption study of 2,4-dichlorophenol on organoclays constructed for soil bioremediation, *Colloids Surf. A* 265 (2005) 81–87.
- [19] G. Akcay, E. Killinc, M. Akcay, The equilibrium and kinetics studies of flurbiprofen adsorption onto tetrabutylammonium montmorillonite (TBAM), *Colloids Surf. A* 335 (2009) 189–193.
- [20] J. Smith, A. Galan, Sorption of nonionic organic contaminants to single and dual organic cation bentonites from water, *Environ. Sci. Technol.* 29 (1995) 685–692.
- [21] L.Z. Zhu, B.L. Chen, X.Y. Shen, Sorption of phenol, p-nitrophenol, and aniline to dual-cation organobentonites from water, *Environ. Sci. Technol.* 34 (2000) 468–475.
- [22] K.L. Lin, J.Y. Pan, Y.W. Chen, R.M. Cheng, X.C. Xu, Study the adsorption of phenol from aqueous solution on hydroxyapatite nanopowders, *J. Hazard. Mater.* 161 (2009) 231–240.
- [23] G. Dursun, H. Cicek, A.Y. Dursun, Adsorption of phenol from aqueous solution by using carbonized beet pulp, *J. Hazard. Mater.* 125 (2005) 175–182.
- [24] Q. Jiang, C. Cooper, S. Ouki, Comparison of modified montmorillonite adsorbents. Part I. Preparation, characterization and phenol adsorption, *Chemosphere* 47 (2002) 711–716.
- [25] A.H. Gemeay, Adsorption characteristics and the kinetics of the cation exchange of rhodamine-6G with Na<sup>+</sup>-montmorillonite, *J. Colloid Interface Sci.* 251 (2002) 235–241.
- [26] C.H. Wu, Adsorption of reactive dye onto carbon nanotubes: equilibrium, kinetics and thermodynamics, *J. Hazard. Mater.* 144 (2007) 93–100.
- [27] F. Spurlock, J. Biggar, Thermodynamics of organic chemical partition in soils. 2. Nonlinear partition of substituted phenylureas from aqueous solution, *Environ. Sci. Technol.* 28 (1994) 996–1002.
- [28] Y. Yu, Y. Zhuang, Z. Wang, Adsorption of water-soluble dye onto functionalized resin, *J. Colloid Interface Sci.* 242 (2001) 288–293.